Journal of Thermal Analysis and Calorimetry, Vol. 70 (2002) 651–662

MISCIBILITY STUDIES ON CROSS-LINKED EVA/LLDPE BLENDS BY TMDSC

F. Cser[*], *M. Jollands, P. White and S. Bhattacharya*

Rheology and Materials Processing Centre, Department of Chemical and Metallurgical Engineering, RMIT University, GPO Box 2476V, Melbourne, VIC. 3001 Australia

(Received January 12, 2001; in revised form May 24, 2002)

Abstract

Cross-linked polymers have particular rheological responses during reprocessing, e. g. if the material is recycled, special processing conditions are required. Other virgin polymers can be used as a blending component to enhance rheological properties.

Bi-layer film of EVA/LLDPE was produced on a blown film line and cross-linked by high-energy radiation. This film was 'agglomerated' then reprocessed in a twin-screw extruder with virgin LLDPE and blown into film. The miscibility of the blend components was then studied using a TA Instruments temperature modulated differential scanning calorimeter (TMDSC).

It was found that the cross-linked EVA/LLDPE scrap and the LLDPE have a slight miscibility in the liquid state. A bigger portion of LLDPE was miscible (dissolved) in EVA in low LLDPE blends. A positive deviation in the heat capacity of the LLDPE component compared to the additivity rule indicated melting to be more reversible in the first heating cycle. This initial miscibility was attributed to being induced by high shear during processing. A smaller positive deviation also occurred in the second heating cycle. This was attributed to intrinsic miscibility.

Keywords: EVA, LLDPE, miscibility, polyethylene, TMDSC

Introduction

A large amount of polymeric waste is generated as a mixture of polymers, e. g. waste from the production of multi-layer film. This waste is generally less easily recycled than single grade polymer waste. Furthermore, if any of the layers is cross-linked to improve some packaging properties such as shrinkage or resistance to environmental stress cracking [1], it introduces reprocessing problems due to the 'high viscosity' of the cross-linked layer. Adding another polymer to enhance processing or product properties might overcome these problems.

Melt blending of different polymers results in blends, which might be miscible or immiscible or only partly miscible. Miscibility or immiscibility between blending

---

[*] Author for correspondence: E-mail: Ferenc.Cser@RMIT.edu.au

1418–2874/2002/ $ 5.00

Akadémiai Kiadó, Budapest
Kluwer Academic Publishers, Dordrecht

components often results in low mechanical properties of the blends, which are then not satisfactory for commercial purposes. To promote suitable polymer-polymer interactions in immiscible blends, compatibilizers are often employed.

Phase interaction (in particular miscibility) in blends can be studied by thermoanalytic methods. A variation in the glass transition temperature correlates with the degree of miscibility of amorphous components but is often too small to measure accurately. The melting temperature of the crystallites in semicrystalline polymers, is a better indication of the solubility – and consequently the miscibility – of the components. Both of the components being semicrystalline give the best chance to analyse their miscibility. Melting point depression points to the dissolution of the crystals of one component in the liquid of the other component, suggesting that some kind of miscibility would also occur in the liquid phase [2]. Blends comprising ethylene-vinyl acetate copolymer (EVA) and various types of polyethylene (low, linear low and high-density polyethylene i.e. LDPE, LLDPE and HDPE) have been found to be immiscible [3, 4]. In blends of EVA and HDPE the EVA formed fine domains in the HDPE.

It has also been observed that miscibility of a blend can be changed when the polymers are sheared [5–8]. Takahashi *et al*. [9] reported the formation of completely miscible blends from completely immiscible polymers at very high shear stresses. It has also been established that the best shear mixing is achieved with blend components of similar viscosity.

Work on films produced from blends comprising cross-linked EVA/LLDPE scrap and virgin LDPE and LLDPE in our laboratories were previously reported [10]. Polarising microscope micrographs did not reveal a structure with obvious phase separation. Barely discernible phase boundaries suggested that the virgin LDPE might be miscible with cross-linked EVA, i.e. it had been incorporated/dissolved into the cross-linked gel. This was unexpected and further investigations of the miscibility of the polymer blend using temperature modulated differential scanning calorimetry (TMDSC) showed some degree of miscibility of cross-linked EVA/LLDPE scrap with LDPE [10]. However LLDPE was found, to be immiscible.

This paper discusses the further study of miscibility of a cross-linked EVA/LLDPE with uncrosslinked (virgin) LLDPE. A series of blend concentrations were studied using TMDSC. The components of the blends were scrap obtained from cross-linked EVA/LLDPE multilayer film and a virgin LLDPE.

Experimental

Materials

The polymeric blends used in this study consist of cross-linked EVA and LLDPE blended with virgin LLDPE. The virgin materials are listed in Table 1, their heat of fusion are given in Table 2. The cross-linking of amorphous regions in our particular case is not dense, yielding about 75 mass% gel content in tests according ASTM D2765 [11]. However, the gel content alone does not reveal the cross-link density. Due to the high flexibility of the film it can be deduced that the cross-link density, i.e. amount of cross-links per chain length unit, is fairly low.

Table 1 Material characterisation of used polymer blend ingredients

Material codes	Material	Co-monomer	Density/g cm^{-3}	MFI/g 10 min^{-1}
EVA	EVA	vinyl acetate	0.911	6.6
LLDPE1	LLDPE	hexane	0.921	0.3
LLDPE2	LLDPE	hexane	0.921	2.5

Table 2 Heat of fusion values for the virgin materials

Material codes	Total melting enthalpy/J g^{-1}	
	1st heating cycle	2nd heating cycle
EVA	122	108
LLDPE1	106	97
LLDPE2	145	147

Methods

The blends were prepared using a Brabender 7L/D twin-screw laboratory extruder at 130 rpm, with set temperatures 130°C for all zones.

Film was blown from the blends using a laboratory scale single-screw extruder of Strängplast type (22L/D) at 150°C with 55 rpm producing film of 65 μm thickness.

Polymer miscibility can be tested using a range of different techniques such as optical and X-ray diffraction, microscopic, spectroscopic, thermographic or thermomechanical techniques. For this study a temperature modulated differential scanning calorimetry (TMDSC) equipped by an RCS unit from TA Instruments was employed.

Two complete heating and cooling cycles between –10 and 190°C were run at heating and cooling rates of 2°C min^{-1}. The modulation amplitude was 0.6°C and the modulation period was 40 s. This is a medium depth of modulation, *i.e.* there is cooling during heating and reverse. Helium was used as a purge gas at a constant flow rate of 30 mL min^{-1}. Nitrogen was used as a heat transfer gas with 100 mL min^{-1} flow rate running through RCS cooling device. Samples for TMDSC tests were cut from the blown film having a mass of approximately 10 mg with an overall thickness of 0.2 mm.

The heat of fusion was obtained from the total heat flow curves by integration. Both the lower and upper limits of integration were taken when the heat capacities obtained on cooling joined those obtained on heating (~10 and ~125°C) [11]. The reproducibility of heat flow (J g^{-1}) in TMDSC is better than 3% and in melting peak temperature is ±0.1°C [12].

Results

Figure 1 shows the total heat flow curves and Fig. 2 the corresponding heat capacity curves for the scrap recorded in the first and the second heating and cooling runs. The heats of fusion are given in Table 3; the peak melting temperatures are given in Table 4.

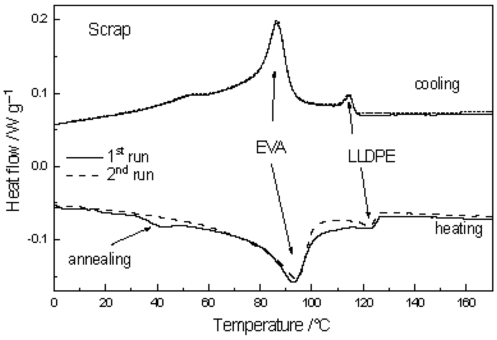

Fig. 1 Total heat flow curves of the scrap. Endothermic heat flow is downwards

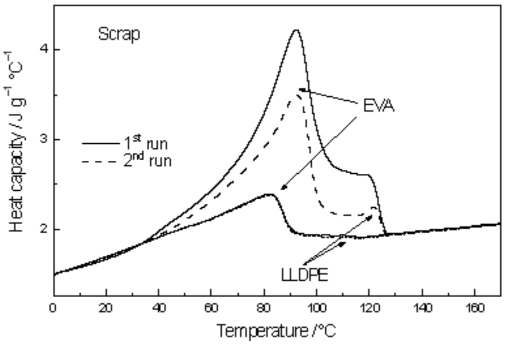

Fig. 2 Heat capacity curves of the scrap

Table 3 Heat of fusion in J g^{-1} of the samples in the first and in the second heating runs

LLDPE2/%	1st heating run			2nd heating run		
	Total	EVA*	LLDPE*#	Total	EVA*	LLDPE*#
0	101.9	67.0	2.6	100.0	100.0	3.6
20	112.6	23.5	22.9	101.0	31.37	21.8
40	124.6	23.7	34.5	112.5	22.49	34.1
60	133.2	5.2	54.2	120.9	7.776	55.9
80	104.8	0.9	69.7	131.3	1.439	72.5
100	145.2	0	145.2	146.5	0	146.5

*The heat of fusion for the individual components is under estimated due to the lack of the proper separation of the peaks corresponding to the components

#Including the values of both types of LLDPE

Table 4 The peak melting temperatures of the components within LLDPE/scrap blends given in (°C)

LLDPE2/%	1st heating run		2nd heating run	
	EVA	LLDPE	EVA	LLDPE
0	93.21	123.66	93.59	122.27
20	92.56	124.19	93.53	124.94
40	91.65	124.32	93.62	125.15
60	91.23	124.37	92.45	125.27
80	91.51	124.50	92.02	125.16
100	–	124.52	–	125.14

The first heating cycle gives us mixed information on the thermodynamic state of the system. It reflects the current thermodynamic state of the system as well as the thermal history. There is a broad peak in the total heat flow curve at 40°C. This is an annealing effect that occurs in semicrystalline systems when they were kept above the starting temperature of the melting transition, which is below room temperature in this particular system. The annealing temperature is present as a step in the heat capacity curve for the first heating as well. Below this temperature the heat capacity curve has a slightly lower value than that of the next cooling and heating runs. As expected, this peak and step are absent on curves recorded in the second heating run, as the thermal history is erased.

Two transition peaks follow that are characteristic of EVA and LLDPE. The PE crystals melt at 95°C in the EVA and at 121°C in the crosslinked LLDPE. The peak melting temperatures of both phases are shifted in the second heating run to a higher value with respect to the first heating run and are also further apart (Table 4).

There are two peaks in the cooling runs corresponding to the crystallisation of polyethylene crystals from the independent phases of EVA and LLDPE.

The total heat flow curves for virgin LLDPE are shown in Fig. 3, the corresponding heat capacity curves are represented in Fig. 4. There is no observable an-

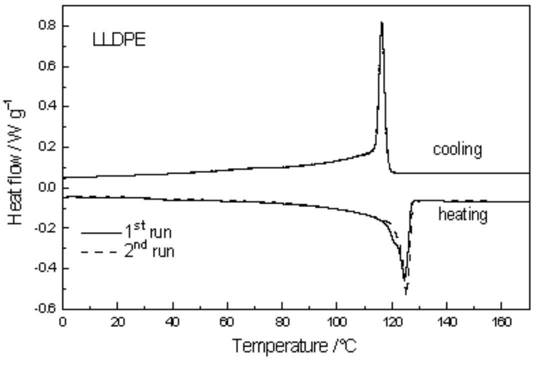

Fig. 3 Total heat flow curves of LLDPE. Endothermic heat flow is downwards

nealing peak in this particular system. The peak melting temperature shifted from 124.5 in the first heating run to 125.1°C in the second one. The melting peak in the second heating run is sharper than that in the first one. The heat capacities obtained from the second heating run have a bimodal character, which is behaviour typical of branched polyethylene.

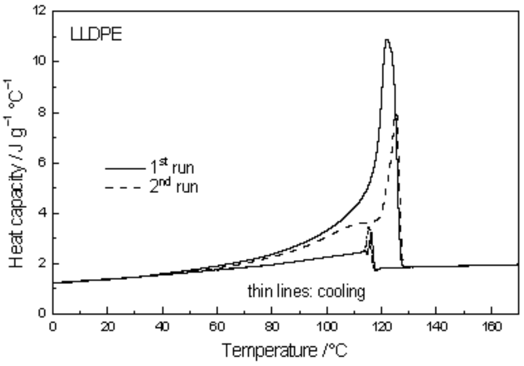

Fig. 4 Heat capacity curves of LLDPE

Total heat flow curves of the LLDPE/scrap blends measured in the first heating and cooling runs respectively are shown in Fig. 5, those of the second heating runs are presented in Fig. 6. The second cooling runs are not shown as they were carbon copies of the first of each sample. The curves show neatly how the TMDSC signal is proportional to the concentration. The curves show clearly the individual character of the two phases, suggesting complete immiscibility. Similarly, the heat capacity curves also show that the changes of the individual peaks are independent (Figs 7 and 8). The LLDPE part of the scrap can be seen in the scrap, i.e. '0% LLDPE' sample. In the blends it is indistinguishable from the melting or crystallisation peaks of the added LLDPE.

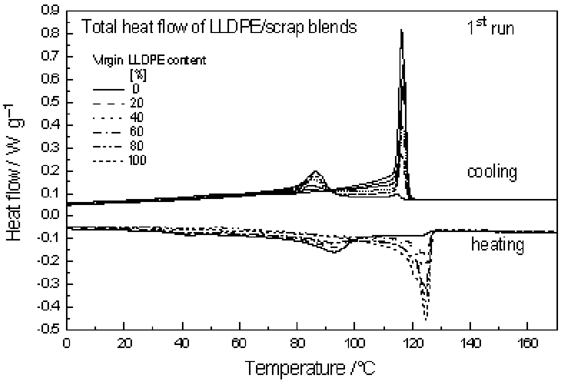

Fig. 5 Total heat flow curves of the scrap/LLDPE mixtures. First heating and cooling runs. Endothermic heat flow is downwards

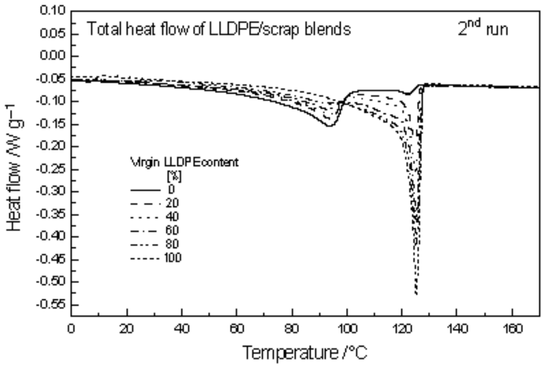

Fig. 6 Total heat flow curves of the scrap/LLDPE mixtures. Second heating runs. Endothermic heat flow is downwards

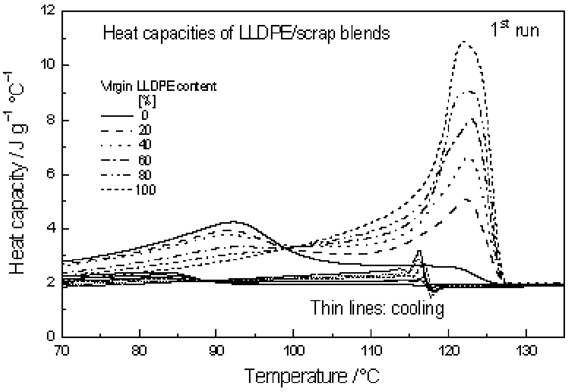

Fig. 7 Heat capacity curves of scrap/LLDPE mixes. First run

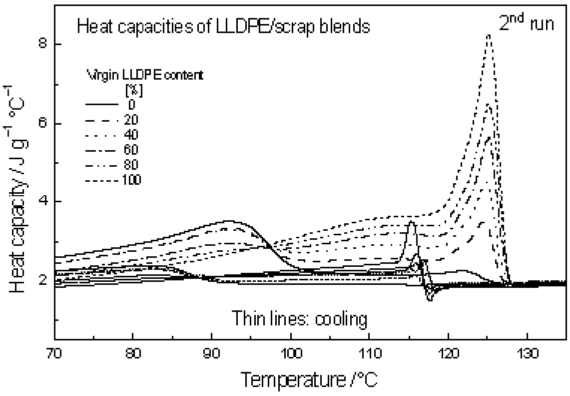

Fig. 8 Heat capacity curves of scrap/LLDPE mixes. Second run

The melting and crystallisation temperatures of the individual peaks (onsets and peaks) are represented as a function of the composition in Figs 9 and 10. The onset and peak temperatures of the virgin LLDPE component are independent of the composition; the temperatures of the EVA part, however, show significant composition dependence. In Fig. 9 the EVA onset of melting temperature increases with increasing LLDPE content in the blend in both heating runs; the corresponding peak temperature slightly decreases in both heating runs. In Fig. 10 the crystallisation temperature (both onset and peak) of the EVA component shifts to lower values with increasing LLDPE content.

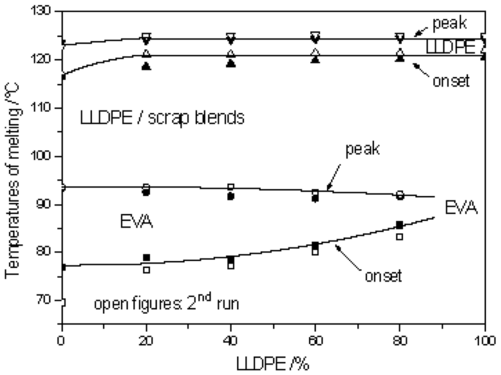

Fig. 9 Change of the onset and the peak temperatures of melting for EVA and LLDPE in the blends. Open figures: first heating run, close figures: second heating run

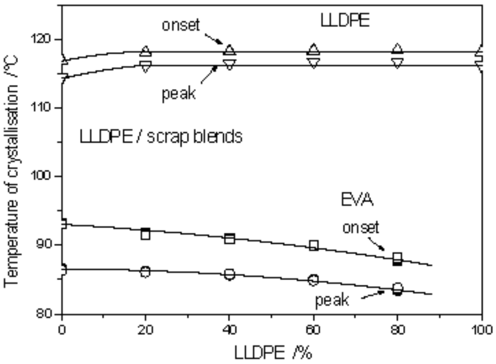

Fig. 10 Change of the onset and the peak temperatures of crystallisation for EVA and LLDPE in the blends. Open figures: first cooling run, close figures: second cooling run

As the geometry of the samples was very similar and eminently suited to a TMDSC study, the additivity of the thermographic curves was tested to further reveal evidence for immiscibility. Figures 11 to 14 show the measured curves of heat capacities compared to those calculated from the base components using the additivity rule. Only heating runs were compared and are represented in the figures.

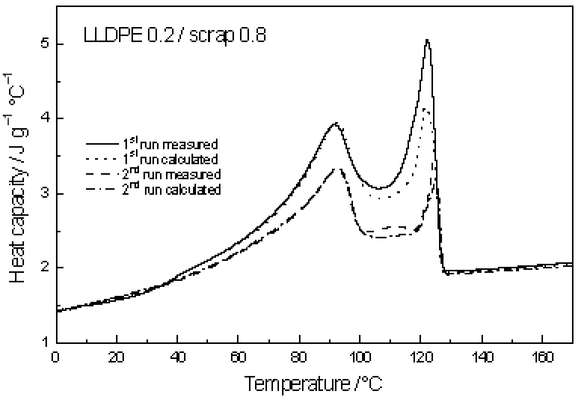

Fig. 11 Measured and calculated heat capacity curves for the mixture with 80% of scrap

Figure 11 shows that the measured and the calculated heat capacity curves for a blend with 20% of LLDPE were identical up to slightly above the peak melting temperature of EVA, i.e. up to 97°C. At higher temperatures the measured curves showed higher heat capacities for the whole range of melting peak of the LLDPE, particularly in the first heating run. A similar kind of deviation was observed for the other compositions, although the differences decreased with increasing LLDPE content. The measured and the calculated total heat capacity curves were nearly identical in the blend with 80% of LLDPE as shown in Fig. 14. Contrary to the trend observed in the LLDPE component, the measured heat capacity curve for the EVA part showed lower values than the calculated ones, and the difference increased with LLDPE content. The peak positions were also shifted to lower temperatures. These changes are very small but significant [12].

The calculated and the measured total heat flow curves were also compared. Small deviations were found, similar to that described above, so the curves are not shown here.

The heat of fusion of the individual components and those of the blends are given in Table 3. The total heat of fusion (shown in columns 2 and 5) was calculated by integrating the whole range of transition, i.e. from 40°C to the end of the melting peak (generally to 130°C). This value is characteristic of the blend as a whole. The heat of fusion of the components are integrated from the onset of the individual peaks using the total heat flow curve as a base line; they are therefore underestimated as the heat flow curves of the components were not able to be de-convoluted. There was no trend in the heat of fusions of the components; they were approximately additive.

Discussion

At first sight the thermodynamic system looked to be an immiscible system of the two phases: the peaks appeared to be independent in both the heat flow and heat capacity curves. However analysis of the onset and the peak temperatures of fusion as well as of crystallisation showed well defined changes that were a function of the composition for the EVA component. This kind of change in the onset and peak temperature of melting of a crystal is well known in eutectic systems. The concept of the eutectic, however, cannot be applied here as both components have the same material in the crystals; they differ only in some characteristics of the crystalline sizes, not in their crystal system or in their composition.

The similarities to the eutectic can, however, be utilised here. The influence of the individual components can be found in the liquid phase from where the polyethylene crystals of the EVA form. When we find any influence of the LLDPE on the crystallisation of the polyethylene in the EVA phase, we can conclude that at least part of the LLDPE must be present in the liquid surrounding the crystals forming from EVA. This means a portion of the virgin LLDPE is miscible (dissolved) with the EVA part of the scrap. As the EVA is cross-linked, it cannot be dissolved in an LLDPE phase but it can dissolve the LLDPE in its phase.

Figures 11 to 14 support this conclusion. There is a positive deviation in the heat capacities of the LLDPE components with respect to the additive rule indicating the melting to be more reversible in the measured system than in the estimated ones. This means that there is an increased solubility of the LLDPE crystals in the liquid phase

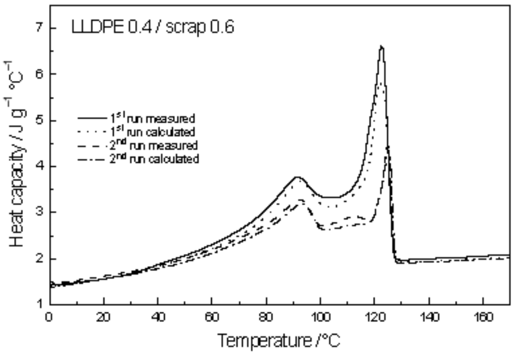

Fig 12 Measured and calculated heat capacity curves for the mixture with 60% of scrap

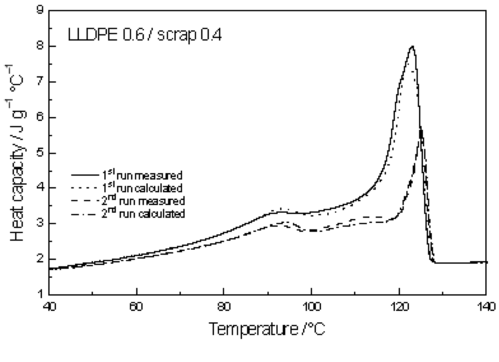

Fig. 13 Measured and calculated heat capacity curves for the mixture with 40% of scrap

of EVA in the presence of LLDPE. The deviation was largest in the high EVA blends because at low level of LLDPE a bigger portion can be dissolved in the EVA. The phenomenon has not been previously reported to the authors' knowledge.

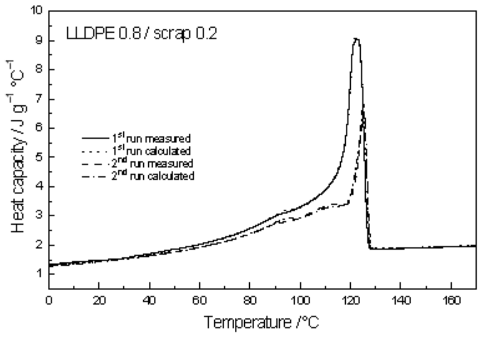

Fig. 14 Measured and calculated heat capacity curves for the mixture with 20% of scrap

The opposite trend was apparent in the EVA component. The deviation was negative and larger in high LLDPE blends. This means that the melting is less reversible in the measured system. The melting peak is also narrower indicating also that the melting is less reversible. These trends are interesting but so small that they are hard to separate from experimental error and have no obvious explanation.

The observed differences between 1st and 2nd heating shows that part of the increased reversibility in the measured system was due to shear mixing; the smaller increased reversibility in the 2nd heating means that part was due to intrinsic miscibility.

Conclusions

Cross-linked EVA/LLDPE scrap dissolves a small amount of virgin LLDPE during shear mixing. Some portion of the virgin LLDPE remains in the EVA phase following phase separation during cooling.

The TMDSC technique can be used to detect liquid phase partial miscibility of similar systems utilising the comparability of the measured data to those calculated on the base of the additivity rule.

References

1 B. Schneier, Crosslinked Thermoplastics, in Handbook of Thermoset Plastics, 2nd. Ed. Noyes Pub. Westwood, N. Y. 1998, p. 498.
2 P. J. Flory, Principles of Polymer Chemistry, N. Y. 1953.
3 R. M. Patel, P. Saavedra, J. deGroot, C. Hinton and R. Guerra, Antec'97, II Hanser, N. Y. (1997).
4 L. A. Utracki, Polymer Alloys and Blends: Thermodynamics and Rheology, 1990.
5 L. An, A. Hinrichs, R. Horst, C. Krause and B. A. Wolf, Macromolecular Symposia, 149 (2000) 75.

6 M. L. Fernandez and J. S. Higgins, Macromolecular Symposia, 98 (1995) 985.

7 I. A. Hindawi, J. S. Higgins and R. A. Weiss, Polymer, 33 (1992) 2522.

8 H. W. Kammer, C. Kummerloewe, J. Kressler and J. P. Melior, Polymer, 32 (1991) 1488.

9 H. Takahashi, T. Matsuoka, T. Ohta, K. Fukumori, T. Kurauchi and O. Kamigaito, J. of Applied Polymer Sci., 36 (1988) 1821.

10 M. G. Sittel-Faraj, F. Cser, M. Jollands and S. Bhattacharya: ANTEC'01, (2001) 2718.

11 ASTM D2765 (1990).

12 F. Cser, F. Rasoul and E. Kosior, J. Therm. Anal. Cal., 50 (1997) 727.

13 L. H. Sperling, Interpenetrating Polymer Networks: An Overview, in Interpenetrating Polymer Networks, 1994, p. 3.